JCI insight

# Erythematous capillary-lymphatic malformations mimicking blood vascular anomalies

René Hägerling, … , Pia Ostergaard, Peter S. Mortimer

*JCI Insight.* 2023. https://doi.org/10.1172/jci.insight.172179.

**Research** In-Press Preview **Angiogenesis** **Cell biology**

## Graphical abstract

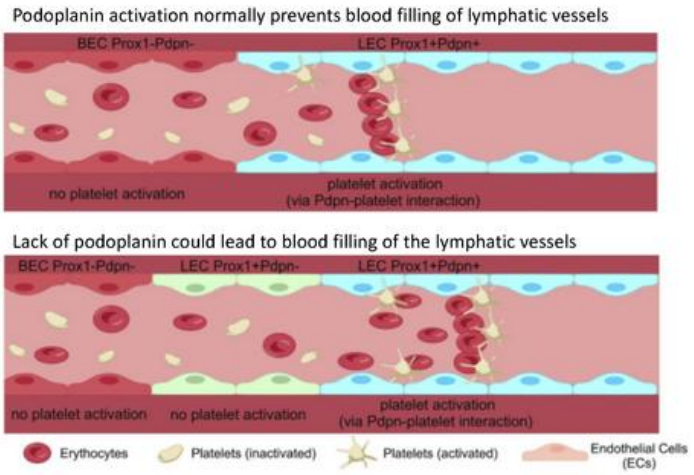

# Erythematous capillary-lymphatic malformations mimicking blood vascular anomalies.

René Hägerling* 1-4,‡, Malou Van Zanten* 5,6, Rose Yinghan Behncke1,2, Sascha Ulferts1,2, Nils R Hansmeier1-4, Bruno Märkl7, Christian Witzel8, Bernard Ho6, Vaughan Keeley9, Katie Riches9, Sahar Mansour5,10, Kristiana Gordon5,6, Pia Ostergaard5, Peter S Mortimer5,6

1. Institute of Medical and Human Genetics, Charité – Universitätsmedizin Berlin, Corporate Member of Freie Universität Berlin and Humboldt-Universität zu Berlin, Augustenburger Platz 1, 13353 Berlin, Germany
2. Berlin Institute of Health at Charité – Universitätsmedizin Berlin, BIH Center for Regenerative Therapies, Augustenburger Platz 1, 13353 Berlin, Germany
3. Berlin Institute of Health at Charité – Universitätsmedizin Berlin, BIH Academy, Clinician Scientist Program, Charitéplatz 1, 10117 Berlin, Germany
4. Research Group Development and Disease, Max Planck Institute for Molecular Genetics, Ihnestrasse 63, 14195 Berlin, Germany
5. Molecular and Clinical Sciences Institute, St George's University of London, London SW17 0RE, UK
6. Dermatology and Lymphovascular Medicine, St George's University Hospitals NHS Foundation Trust, London SW17 0QT, UK
7. Institute of Pathology and Molecular Diagnostics, University Clinic Augsburg, Stenglinstrasse 2, 86156 Augsburg, Germany
8. Department of Surgery, Campus Charité Mitte and Campus Virchow-Klinikum, Charité - Universitätsmedizin Berlin, Corporate Member of Freie Universität Berlin, Humboldt-Universität zu Berlin and Berlin Institute of Health, 10117 Berlin, Germany.

9. Lymphoedema Clinic, Derby Hospitals Foundation NHS Trust, Derby, UK

10. SW Thames Regional Centre for Genomics, St George's University Hospitals NHS Foundation Trust, London, UK

* Shared authorship

‡ Corresponding author:

René Hägerling, Rene.Haegerling@charite.de

Telephone: +49-30-450-569-119

Institute of Medical and Human Genetics, Charité – Universitätsmedizin Berlin, Corporate Member of Freie Universität Berlin and Humboldt-Universität zu Berlin, Augustenburger Platz 1, 13353 Berlin, Germany

**ORCID IDS:**

| | |
|---|---|
| René Hägerling | 0000-0002-6830-2043 |
| Nils Rouven Hansmeier | 0000-0001-7024-5351 |
| Bruno Märkl | 0000-0002-7704-850X |
| Kristiana Gordon | 0000-0002-7840-5644 |
| Sahar Mansour | 0000-0001-6629-4118 |
| Peter Mortimer | 0000-0003-1901-6849 |
| Pia Ostergaard | 0000-0002-2190-1356 |
| Malou van Zanten | 0000-0001-9620-075X |
| Bernard Ho | 0000-0003-2571-3966 |
| Rose Yinghan Behncke | 0009-0005-8503-3411 |
| Sascha Ulferts | 0009-0006-3861-4966 |
| Christian Witzel | 0000-0003-4819-9381 |

**Word count:** 6438

**Keywords:**

Lymphoedema, lymphatic malformation, lightsheet imaging, lymphangiogenesis, vascular malformation, WILD Syndrome, segmental overgrowth

**Number of tables:** 1

**Number of figures:** 6

**ABSTRACT**

Superficial erythematous cutaneous vascular malformations are assumed to be blood vascular in origin, but cutaneous lymphatic malformations can contain blood and appear red. Management may be different and so an accurate diagnosis is important. Cutaneous malformations were investigated through 2D-histology and 3D-whole-mount-histology. Two lesions were clinically considered as port-wine birthmark, and another three lesions as erythematous telangiectasias.

The aims were: i) to prove that cutaneous erythematous malformations including telangiectasia can represent a lymphatic phenotype, ii) to determine if lesions represent expanded but otherwise normal or malformed lymphatics, and iii) to determine if the presence of erythrocytes explained the red colour. Microscopy revealed all lesions as lymphatic structures. Port-wine birthmarks proved to be cystic lesions, with non-uniform lymphatic marker expression, and a disconnected lymphatic network suggesting a lymphatic malformation. Erythematous telangiectasias represented expanded but non-malformed lymphatics. Blood within lymphatics appeared to explain the colour. Blood-lymphatic-shunts could be detected in the erythematous telangiectasia.

In conclusion, erythematous cutaneous capillary lesions may be lymphatic in origin but clinically indistinguishable from blood vascular malformations. Biopsy is advised for correct phenotyping and management. Erythrocytes are the likely explanation for colour accessing lymphatics through lympho-venous-shunts.

## INTRODUCTION

There is a general assumption that a erythematous cutaneous vascular malformation (naevus) is a disorder of dermal blood vessels. Rarely is consideration given to the possibility that they may represent a lymphatic structure. This may have implications for phenotyping and management.

In his 2015 classification of capillary malformations, Happle makes no mention of cutaneous lymphatic malformations that may be red. The assumption would be that they are blood vascular malformations (1). In the clinic, differentiation may be relatively straightforward in a classic 'lymphangioma circumscriptum' containing blood, but not so in other cutaneous lymphatic malformations that are red.

In the ISSVA classification of capillary malformations no consideration is given to the fact that cutaneous erythematous naevi or erythematous cutaneous telangiectasia may be lymphatic in origin nor in the classification of lymphatic malformations is mention made of cutaneous involvement as a red 'birthmark' (2).

We describe 5 cases, two displaying port-wine birthmarks (or naevus flammeus) and three exhibiting erythematous cutaneous telangiectasia, where the clinical diagnosis was a (blood) capillary malformation, but all proved with histological analysis to be a lymphatic vessel structure.

The purpose of the communication is:

1. To determine if cutaneous erythematous malformations including port-wine birthmarks and telangiectasia can represent a lymphatic phenotype.

2. To determine if the lesions represent expanded, but otherwise normal dermal lymphatic vessels, or malformed lymphatics.

3. To determine if the presence of red blood cells was the explanation for the red colour.

For this purpose, we have performed classical 2D histological analysis as well as whole-mount 3D histology. In contrast to physical sectioning in 2D histology approaches, 3D histology represents a light sheet imaging based optical sectioning methodology, which allows generation of series of optical sections from immunofluorescence stained, optically cleared tissue samples (3–5). Following digital 3D reconstruction of the optical sections, the entire lymphatic vascular network is visualized in 3D space. Therefore, 3D histology represents a brilliant tool for vascular phenotyping and in-depth understanding of the underlying vascular alterations.

## RESULTS

Presented here are five cases of erythematous cutaneous capillary malformations which clinically would be described as ‘birthmarks’ or naevi. Two cases exhibited port-wine birthmark lesions (cases 1-2) and in three cases dark red telangiectasia were observed in the skin of a swollen thigh (cases 3-5).

Case 1: Segmental overgrowth and vascular malformation (Klippel Trenaunay Syndrome) of right hindquarter (naevus flammeus)

A 24-year-old male was referred for management of swelling of his right leg. He was noted to have obvious varicose veins as well as a port-wine birthmark/naevus flammeus extending up the entire right leg from ankle to groin which had been present since birth. There was pitting oedema detectable in the right leg and foot but not the left leg which was normal. There was

no limb length discrepancy although his right leg was slightly bigger in girth than the left leg. He had been diagnosed as Klippel-Trenaunay syndrome (KTS) (Figure 1 A-B). Lymphoscintigraphy showed mild abnormalities of lymphatic function. A skin biopsy was obtained from the affected leg. No post-zygotic mosaic pathogenic variants were detected in the *PIK3CA* gene, nor any of the genes in the AKT pathway nor the RAS/MAPKinase pathway.

2D histology: Haematoxylin-Eosin (H&E) staining of the specimen revealed no obvious lymphatic or blood vascular alteration (Figure 1C). Immunofluorescence staining of sections for the pan-endothelial marker CD31 as well as the lymphatic vessel marker Podoplanin (PDPN) showed presence of lymphatic and blood vessels but did not provide any further information on a possible lymphatic phenotype or the origin of the red colour of the lesion (Supplemental Figure 1A-D).

Whole-mount 3D histology: Analysis of the acquired 2D optical sections of the affected tissue biopsy showed dilated, vascular cystic lesions in the papillary dermis (Figure 1D). The cystic lesions showed strong expression of the lymphatic markers Prox1 and Podoplanin indicating a lymphatic vascular origin of the naevus flammeus. However, further detailed examination of the expression of Prox1 and Podoplanin in all optical sections revealed a non-uniform expression of Podoplanin, whereas Prox1 expression was unaltered (Figure 1D, white arrow). In addition, red blood cells were detected within Prox1-positive, Podoplanin-positive vessels using autofluorescence (Figure 1D, white arrow heads).

The 3D reconstruction of the entire biopsy provided additional information on the lymphatic phenotype. In contrast to the area in the papillary dermis showing Podoplanin-negative, Prox1-positive lesions (Figure 1E-G, red arrows), deeper lymphatic vessels in the dermis showed no presence of cystic lymphatic lesions and only few dilated lymphatic vessels. In the lymphatic

vasculature of the deeper dermis no lymphatic valves were detected (data not shown). Non-connected lumenised lymphatic vessels were detected in the dermis (Figure 1E-H, red arrow heads). En-face view of the lymphatic cystic lesions directly underneath the epidermis showed the non-uniformly distributed presence of microcysts (Figure 1H).

Case 2: Segmental overgrowth and vascular malformation of the left fore-quarter (naevus flammeus)

A 24-year-old male had lymphoedema and overgrowth of his left upper limb and scapula from birth. Extensive port-wine birthmarks were present on both legs, upper torso, right upper arm, and neck. There was no segmental overgrowth of the lower limbs, but there were extensive venous varicosities and engorgement (Figure 2A-B). The right foot was slightly swollen with 2-3 syndactyly. On venous duplex ultrasound there was incompetence of deep veins, posterior tibial vein, and peroneal vein as well as the long saphenous and perforating veins seen in the right leg. In the left leg, there was incompetence of the short saphenous and perforating veins only. DNA was extracted from a skin biopsy of the affected limb. No post-zygotic mosaic pathogenic variants were detected in the *PIK3CA* gene, nor any of the genes in the AKT pathway nor the RAS/MAPKinase pathway.

2D histology: no discrimination between lymphatic and blood vessel phenotype could be detected in H&E staining (Figure 2C). The Immunofluorescence staining for blood (CD31) and lymphatic vessel markers (Podoplanin) showed presence of lymphatic vessels and normal blood vessels. No erythrocytes could be detected within lymphatic vessels (Supplemental Figure 1E-H).

Whole-mount 3D histology: analysis of the optical sections revealed the presence of dilated, hyperplastic lymphatic vessels located in the papillary dermis (Figure 2D). In accordance with the findings in Figure 1D, a non-uniform expression of Podoplanin in the vessels was detected. Strong Prox1 expression is not altered in these vessels (Figure 2D, white arrows). The presence of blood filled Podoplanin-positive, Prox1-positive vessels was detected using autofluorescence (Figure 2D, white arrowhead).

The 3D reconstruction of the entire biopsy provided additional information on the lymphatic phenotype. In contrast to the area in the papillary dermis showing Podoplanin-negative, Prox1-positive lesions (Figure 1E-G, red arrows), deeper lymphatic vessels in the dermis showed no presence of cystic lymphatic lesions and only few dilated lymphatic vessels. In the lymphatic vasculature of the deeper dermis no lymphatic valves were detected. Non-connected lumenised lymphatic vessels were detected in the dermis (Figure 2E-H, red arrow heads). En-face view of the lymphatic cystic lesions in the papillary dermis showed the non-uniformly distributed presence of microcysts (Figure 2H, white arrows).

Case 3: WILD syndrome (erythematous telangiectasia)

A 11-year-old male was born with bilateral upper limb primary lymphoedema with ‘boxing glove’ swelling of the hands (Figure 3A), right thigh lymphoedema, genital lymphoedema as well as widespread cutaneous lymph blisters (lymphangiectasia) particularly on the trunk, and scattered red spider-like capillaries also in the skin (Figure 3B). No segmental overgrowth was observed and no venous problems reported. He has been given a working diagnosis of WILD syndrome (Warts, Immunodeficiency, Lymphatic Dysplasia) (6, 7). The erythematous telangiectasia appeared evanescent as they could come and go over weeks of observation. One of the erythematous telangiectasia was biopsied. The genetic cause of WILD syndrome has not

yet been identified so whole genome sequencing (as part of the Genomics England's 100,000 Genomes Project) was performed but no pathogenic variants were identified. Mosaicism is suspected and genetic analysis is being performed on DNA from skin fibroblasts as part of an on-going research study to identify the cause of WILD syndrome.

2D histology: H&E staining showed dilated vascular lumens, most likely lymphatic vessels (Figure 3C and Supplemental Figure 1I-L).

Whole-mount 3D histology: Analysis of the acquired 2D optical sections of the affected tissue biopsy showed dilated weak Prox1-positive, strong PDPN-positive vessels in the area of the papillary dermis (Figure 3D, red arrows), but no cystic vascular structures. The lymphatic vessel density appeared increased compared to healthy control samples (Supplemental Figure 2). Further detailed examination of the expression of Prox1 and Podoplanin in all optical sections revealed a uniform, non-altered expression of Podoplanin and Prox1.

The 3D reconstruction of the entire sample provided additional information on lymphatic vessels. In contrast to the lymphatic vasculature in normal skin, the visualised lymphatic vasculature did not show hierarchical organisation of the vascular tree but hyperplastic, dilated lymphatic vessels in the deeper dermis (Figure 3E-G). Non-connected, lumenised vessel fragments were present (Figure 3E, G-H, red arrow heads). In contrast to the papillary dermis (Figure 3E-G, white arrow), Prox1 was expressed only weakly (Figure 3F-G). In the lymphatic vasculature of the deeper dermis no lymphatic valves were detected.

<u>Case 4: WILD syndrome (erythematous telangiectasia)</u>

A 21-year-old female presented with pubertal onset swelling of her left leg, consistent with primary lymphoedema. The lymphoedema extended into the left flank and buttock but there

was no limb length discrepancy. No segmental overgrowth was observed and no venous problems reported. She had hypertrophy/oedema of the left breast. She had what was considered a cutaneous vascular malformation on both sides of her neck and there were two small telangiectasias on her left thigh (Figure 4A). Lymphoscintigraphy showed re-routed lymph drainage through the deep system via popliteal nodes but with normal levels of transport in the non-swollen left leg, and functional aplasia in the swollen right leg (Figure 4B). A working diagnosis of WILD syndrome was made (6). Genetic analysis is being performed on DNA from skin fibroblasts as part of an on-going research study to identify the cause of WILD syndrome.

2D histology: H&E staining as well as staining for lymphatic vessel markers revealed no obvious vascular alteration (Figure 4C and Supplemental Figure 1M-P).

Whole-mount 3D histology: In comparison to healthy control (Supplemental Figure 2), 3D-histology of the entire lymphatic vasculature as shown in 2D (Figure 4D) as well as 3D (Figure 4E-H) revealed a normal, non-dilated lymphatic vessel architecture and low Prox1 expression. A very low number of valves was detectable compared to control samples (Supplemental Figure 2). Neither cystic vascular lesion nor non-connected vessel fragments were detected. However, a Podoplanin-positive lymphatic vessel which is packed with erythrocytes were seen (Figure 4D, white arrowhead), indicating possible connections between lymph and blood vessels. On closer inspection, erythrocytes, highlighted by autofluorescence, were observed within unstained blood vessels draining into Podoplanin-positive lymphatic vessel (Supplemental Figure 3). This indicated a potential shunting site, which could not be investigated further with the current material.

Case 5: WILD syndrome (erythematous telangiectasia)

A 22-year-old female patient presented at birth with lymphoedema of her left lower limb/hindquarter, left upper limb, and left side of the face. No overgrowth was observed and no venous problems reported. Also noted was a cutaneous vascular lesion on the left side of the chest and fixed erythematous telangiectasia on the left thigh (Figure 5A). These abnormalities did not change and had grown with her. Lower limb lymphoscintigraphy revealed reduced lymph node uptake of tracer in the left groin but otherwise normal looking lymph drainage pathways in both legs (Figure 5B) (7). DNA was extracted from blood lymphocytes - no pathogenic variants were identified in a panel of 22 genes known to be associated with lymphatic problems. A diagnosis of WILD syndrome was made based on her clinical features. Genetic analysis is being performed on DNA from skin fibroblasts as part of an on-going research study to identify the cause of WILD syndrome.

2D histology: H&E staining as well as staining for lymphatic vessel markers revealed no obvious vascular alteration (Figure 5C and Supplemental Figure 1Q-T).

Whole-mount 3D histology: A normal lymph vessel network with weak Prox1 expression (Figure 5 D-H). A very low number of lymphatic valves was detectable. No cystic vascular lesions or dilated vessels were detected. Similar to case 4, podoplanin-positive lymphatic vessels packed with red blood cells were observed (Figure 5D, white arrowheads), indicating that the telangiectasias represented lymphatic vessels containing blood hence their red colour.

Blood-lymphatic vessel shunts can be detected in erythematous cutaneous telangiectasia

To further investigate the red colour of the lymphatic vasculature in more detail, a thorough analysis of all optical sections from the light sheet image stacks for the presence of erythrocytes

in lymphatic vessels was performed. In contrast to case 3 (Figure 3D), blood filled lymphatic vessels were identified at multiple positions in case 4 and 5 (Figure 4D and Figure 5D, white arrowheads) using autofluorescence of red blood cells. Following the blood-filled vessels in three-dimensional space revealed a potential connection site between blood vessels and lymphatic vessels resulting in blood-lymphatic shunting (Supplemental Figure 3) and therefore the presence of red blood cells in lymphatic vessels.

## DISCUSSION

Cutaneous erythematous lesions resembling vascular naevi or 'birthmarks' are generally assumed to be blood vascular in origin. Here we describe five erythematous cutaneous vascular malformations on legs of patients with primary lymphoedema. Lesions in two cases were considered to be naevus flammeus and lesions in the other three cases were clinically seen as erythematous telangiectasia. All lesions proved to be lymphatic vessels on histological analysis of biopsies.

Blood is frequently found in abnormal dermal lymphatic vessels and particularly malformations e.g. lymphangioma circumscriptum (8). Blood vessels and lymphatic vessels have the same embryological origins so, in vascular malformations, it may not be surprising if dermal vessels are not fully differentiated and may appear like each other (hybrid). In development, platelets are important for maintaining venous integrity and so, in malformations, lymphatics can be connected to blood vessels resulting in blood shunting from one vessel to the other (9, 10).

Port-wine birthmarks/naevus flammeus are always considered blood vascular in type. As Happle (1) states: “the term capillary malformation is presently used to designate numerous quite different disorders such as port-wine birthmark (naevus flammeus), the salmon patch, the vascular naevus of the ‘megalencephaly-capillary malformation syndrome’ (MCAP) and the skin lesions of other non-hereditary conditions such as ‘capillary malformation-arteriovenous malformation’ (CM-AVM) as well as hereditary traits such as autosomal recessive ‘microcephaly-capillary malformation’ (MICCAP)” (1). There is no mention of lymphatic origin for capillary malformations. The implication is that all capillary malformations are blood vessel in origin but as demonstrated from results presented here, lymphatic capillary malformation should be added. Maari and Frieden in 2004 recognised that some port-wine birthmarks have a strong connection to associated lymphatic disease but there was no histological evidence to support their statement (11).

The 3D histological data from the naevus flammeus presented here showed cystic lesions of a lymphatic malformation of the identified vessels. In contrast, erythematous cutaneous telangiectasia had singular distinct connection sites between blood and lymphatic vessels (in naevus flammeus no distinct connection sites could be detected). A general transition from malformed blood vessels to lymphatic malformations appears to be the most common pattern in the analysed samples.

Telangiectasia simply means ‘end vessel dilatation’ (from Greek: Telos=end; angeion=vessel; ektasis=stretching out, extension, dilatation). Their spidery nature indicates vessels horizontal to the skin surface e.g. spider telangiectasia. The redness is assumed to be from blood cells and telangiectasias are considered to represent expansion of pre-existing blood vessels. However,

the erythematous cutaneous telangiectasias observed here proved to be of lymphatic phenotype on histological analysis.

There are reports of cutaneous capillary-lymphatic malformations (12). Net-like superficial lymphatic malformations have been described and equate to the telangiectatic lymphatic malformations described here. Noguera-Morel et al. described 3 examples of distinctive progressive, superficial red to purple patches composed of an arborizing network of vessels, histologically demonstrating anomalous lymphatics in the upper dermis. They suggest these cases are best considered as a distinct form of Superficial Lymphatic Malformation (13). Vide et al. described one case of a lymphatic malformation in the upper dermis manifesting as transient purple reticulated patches, distinct from those included in the ISSVA classification and distinct from hobnail haemangioma (14). The third published case described red to purplish macules with a finely reticulated pattern of vascular structures. Dermoscopy showed arborizing telangiectatic vessels and biopsy confirmed a lymphatic origin (15).

In all published cases the telangiectasia lesions were not congenital and often transient, remaining in place for a few weeks and then fading away slowly while others appeared in the same area. This was true for our cases of erythematous capillary-lymphatic malformations appearing as telangiectasia. Their behaviour is similar to the reappearing ‘lymph blisters’ seen on the skin surface with a lymphangioma circumscriptum (8). We believe that these erythematous capillary-lymphatic malformations may represent engorgement of dermal lymphatic vessels due to lymph reflux (dermal backflow) from a deeper lymphatic malformation which may be associated with lymphoedema. We hypothesise that as dermal intra-lymphatic pressures rise and fall then the visible nature of these lesions come and go.

But why are these lesions red? Intra-lymphatic blood cells would be one answer, but red cells are not always found on biopsy. Dermal lymphatics can be red if inflamed (lymphangitis). Dermal lymphatics infiltrated by metastatic cancer (lymphangitis carcinomatosis) can present with a similar appearance. Under these circumstances red cells are not observed on biopsy and so redness may be due to mechanisms other than luminal red cells (16). Nevertheless, blood filled lymphatic vessels were identified at multiple positions in cases 4 and 5 using autofluorescence of red blood cells. Following the blood-filled vessels in 3D space revealed a distinct connection site between blood vessels and lymphatic vessels resulting in blood-lymphatic shunting and therefore the presence of red blood cells in lymphatic vessels. Although this would need further investigation using relevant immunofluorescent markers.

What the current study did demonstrate using lymphatic markers was an altered expression of Prox1 and Podoplanin in the malformed vessels. Prox1-positive vessels near blood vessels showed no, or weak, expression of Podoplanin, whereas more distant Prox1-positive vessels express Podoplanin. An important role of Podoplanin, expressed by lymphatic vessels, is in preventing postnatal blood filling of the lymphatic vascular system (17). This is a platelet dependent process (18). Therefore, it is tempting to hypothesise that the altered expression of the lymphatic marker Podoplanin results in blood-filling of lymphatic vessels as Podoplanin signalling has been shown to be essential for platelet activation and separation of blood and lymphatic vessels (17, 18). Due to downregulation of Podoplanin on Prox1-positive lymphatic endothelial cells located next to blood endothelial cells, activation of platelets, while entering Podoplanin-negative lymphatic vessel structures, is impaired (Figure 6). This results in the presence of erythrocytes and white cells in lymphatic vessels. Our hypothesis is supported by studies showing dermal blood lymphatic vascular shunting in Podoplanin, Syk and Clec2 deficient mice (17–19).

From our cases reported here, and those in the literature, it is important to recognize that cutaneous erythematous vascular lesions could be lymphatic in origin. This would have important implications for making a correct diagnosis for phenotyping of patients and for genotyping if appropriate. Treatment with PIK3CA- or Map/Kinase-inhibitors might be appropriate if a somatic mutation is identified (20, 21). It might also have implications for infection risk as lymphatic malformations have a higher incidence of infection (22).

In conclusion, erythematous skin lesions may not be blood vascular in origin. As demonstrated here, cutaneous erythematous capillary malformations can be of a lymphatic, not blood vascular, phenotype. Biopsy and 3D whole-mount investigation is necessary for the distinction between the two. The lymphatic cystic lesions, non-uniform expression of lymphatic vessel markers, and the disconnected lymphatic network within the port-wine birthmarks suggest a malformation, whereas the erythematous telangiectasia seem to represent expanded but not necessarily malformed dermal lymphatic vessels. A erythematous capillary-lymphatic malformation should be considered in vascular anomalies where other lymphatic abnormalities such as lymphoedema are present. Blood is the most likely explanation for the colour which might access the lymphatics through lympho-venous shunts or opening up of lympho-venous anastomoses.

## MATERIAL & METHODS

### Recruitment and biopsy

Two patients with cutaneous erythematous vascular ‘naevus flammeus’ lesions and lower limb primary lymphoedema, and three patients with erythematous telangiectasia and limb lymphoedema were recruited for skin biopsy and histological analysis from two National

Primary Lymphoedema clinics in the UK (Derby and London). 6mm punch biopsies were obtained under local anaesthetic. Beside standard two-dimensional (2D) histology, three-dimensional (3D) histological analysis was performed using light sheet imaging.

Genetic testing

Diagnostic genetic testing in our clinic is performed according to the clinical presentation. For patients with segmental overgrowth and vascular malformations (cases 1 and 2), a skin biopsy of an affected area was obtained, DNA extracted, and screened for post zygotic, mosaic mutations on the overgrowth panel (includes genes in the Akt and RAS MAP kinase pathway) as per standard protocol in the SW Thames Regional Centre for Genomics.

For patients in whom we suspect a germline mutation, we would take blood for the lymphoedema gene panel or whole genome sequencing. The current list of genes on the Genomics England Primary Lymphoedema gene panel (Version 3.2) can be viewed here: https://panelapp.genomicsengland.co.uk/panels/65/.

Antibodies

The following antibodies were used: Mouse monoclonal $IgG_1$ anti-human PODOPLANIN (MA1-83884, Invitrogen, Waltham, MA, USA), rabbit polyclonal IgG anti-human PROX-1 (102-PA32AG, ReliaTech, Wolfenbüttel, DE), donkey polyclonal anti-mouse IgG Alexa Fluor 568 (A10037, Invitrogen, Waltham, MA, USA), donkey polyclonal anti-rabbit IgG Alexa Fluor 488 (A21206, Invitrogen, Waltham, MA, USA).

Standard immunofluorescence histology

Tissue sectioning of tissue samples was performed as described before (4). After fixation of skin biopsies in 4% PFA/PBS for 4 hours, samples were washed in PBS, embedded and snap-

frozen in OCT. 10 μm cryosections were generated. Cryosections were incubated in ice-cold methanol for 15 minutes, washed and blocked (10% chicken serum, 0.3% Triton X-100 in PBS). Following blocking, tissue sections were incubated for 1 hour with primary antibodies (diluted in 1% BSA, 1% chicken serum, 0.3% Triton X-100 in PBS), washed thrice in PBS-T (0.1% Tween20 in PBS) and finally incubated in Alexa dye–conjugated secondary antibodies (Life Technologies). After sample mounting in Mowiol, samples were imaged using a Zeiss LSM 980 confocal microscope (25x oil, NA = 0.8).

Standard histology

Histochemical staining was performed on 5 μm sections. A Ventana BenchMark ULTRA platform was used (Roche, Mannheim, Germany).

Whole-mount skin biopsy immunofluorescence staining for light sheet microscopy

Fresh skin biopsies were fixed in 4% PFA/PBS for 4h at 4°C. Samples were permeabilized (0.5% Triton X-100/PBS), blocked in PermBlock solution (1% BSA, 0.5% Tween 20 in PBS), and whole-mount immunofluorescence staining was performed using indicated primary antibodies and Alexa dye–coupled secondary antibodies diluted in PermBlock solution. Following each staining step, samples were washed thrice in PBS-T (3, 4).

For 3D-histological analysis the entire sample was subjected to whole-mount immunofluorescence staining for the lymphatic markers Prox1 and Podoplanin to detect all the lymphatic vasculature within the specimen.

Optical clearing of whole-mount-stained skin biopsies

Optical clearing of skin samples was performed as described before (3, 4). Briefly, whole-mount immunofluorescence-stained skin biopsies were embedded in 1% low-melting-point agarose and dehydrated in increasing methanol concentrations (50%, 70%, 95%, >99.0%, >99.0% [v/v] methanol, each step 30 minutes). After incubation in a benzyl alcohol/benzyl benzoate (BABB) (ratio 1:2 [v/v]):methanol (>99.0% [v/v]) mixture for 4 hours, samples were incubated in BABB for 4h twice. Optically cleared skin biopsies were stored in BABB for imaging.

Light sheet microscopy, 3D reconstruction and data analysis

Immunofluorescence-stained and optically cleared skin biopsies, were optically sectioned using a LaVision UltraMicroscope II (LaVision BioTec). Image stacks were captured with a step size of 1 μm and at various magnifications. Following imaging, optical sections (>2,000 single optical 2D sections) were digitally 3D reconstructed and analysed. Digital 3D reconstruction of light sheet image stacks was performed using Imaris Microscopy Image Analysis Software (Oxford Instruments, Abingdon, UK) (3, 5).

Ethics approval

Ethical approval was obtained from the local health research authority (REC reference number 12/LO/0498). The study has been conducted according to the principles expressed in the Declaration of Helsinki. All patients provided their written informed consent.

**DATA AVAILABILITY:**

The data that support the findings of this study are available from the corresponding authors upon reasonable request.

**CONFLICT OF INTEREST:**

The authors declare they have no conflict of interest.

**AUTHOR CONTRIBUTIONS:**

Conceptualization and methodology, R.H., M.v.Z., P.O. and P.S.M.; experimentation, R.H., M.v.Z., R.Y.B, S.U. and N.R.H.; data analysis and data curation, R.H., M.v.Z., B.M., R.Y.B.; sample collection, B.H, B.M, C.W.; patient provision, M.v.Z., K.G., S.M., V.K., and K.R.; manuscript preparation, R.H., M.v.Z., K.G., S.M., P.O., P.S.M.; figure preparation and visualization, R.H., R.Y.B., S.U.; project supervision, R.H., P.O., P.S.M; funding acquisition, R.H., K.G., S.M., P.O., P.S.M; All authors have read and agreed to the published version of the manuscript.

**ACKNOWLEDGEMENT:**

We extend our thanks to the patients. We thank Dr. Felix Heymann (Charité – Universitätsmedizin Berlin, Department of Hepatology and Gastroenterology) and Prof. Ansgar Petersen (Berlin Institute of Health Center for Regenerative Therapies (BCRT) at Charité) for support with confocal microscopy and 3D visualization.

**FUNDING:**

This work was supported in part by the Berlin Institute of Health (BIH) and by grants from the Lymphatic Malformation Institute and European Union (ERC, PREVENT, 101078827) (to RH). This work was also supported by a joint grant from the Medical Research Council (MRC) and the British Heart Foundation (BHF) (MR/P011543/1 and RG/17/7/33217) UK.

RH is participant in the BIH-Charité Junior/Digital/Clinician Scientist Program funded by the Charité –Universitätsmedizin Berlin and the Berlin Institute of Health.

**REFERENCES:**

1. Happle R. Capillary malformations: a classification using specific names for specific skin disorders. J Eur Acad Dermatol Venereol. 2015;29(12):2295-2305. doi:10.1111/jdv.13147

2. ISSVA Classification of Vascular Anomalies: International Society for the Study of Vascular Anomalies. Published 2018. Accessed March 16, 2023. https://www.issva.org/classification

3. Hägerling R, et al. A novel multistep mechanism for initial lymphangiogenesis in mouse embryos based on ultramicroscopy. EMBO J. 2013;32(5):629-644. doi:10.1038/emboj.2012.340

4. Hägerling R, et al. VIPAR, a quantitative approach to 3D histopathology applied to lymphatic malformations. JCI Insight. 2017;2(16). doi:10.1172/jci.insight.93424

5. Drees D, et al. Scalable robust graph and feature extraction for arbitrary vessel networks in large volumetric datasets. BMC Bioinformatics. 2021;22(1):346. doi:10.1186/s12859-021-04262-w.

6. Gordon K, et al. Update and audit of the St George's classification algorithm of primary lymphatic anomalies: a clinical and molecular approach to diagnosis. J Med Genet. 2020;57(10):653-659. doi:10.1136/jmedgenet-2019-106084

7. Mansour S, et al. Redefining WILD syndrome: a primary lymphatic dysplasia with congenital multisegmental lymphoedema, cutaneous lymphovascular malformation, CD4 lymphopaenia and warts. J Med Genet. 2023;60(1):84-90. doi:10.1136/jmedgenet-2021-107820

8. Mortimer PS. Disorders of lymphatic vessels. In: Burns T, Breathnach S, Cox NH, Griffiths C, eds. Rook's textbook of dermatology. 8th ed.: Wiley-Blackwell; 2010:48. p. 1–31.

9. Zhang Y, et al. Transient loss of venous integrity during developmental vascular remodeling leads to red blood cell extravasation and clearance by lymphatic vessels. Development. 2018;145(3). doi:10.1242/dev.156745

10. Tucker AB, et al. Lymphovenous shunts: from development to clinical applications. Microcirculation. 2021;28(3):e12682. doi:10.1111/micc.12682

11. Maari C, Frieden IJ. Klippel-Trénaunay syndrome: the importance of "geographic stains" in identifying lymphatic disease and risk of complications. J Am Acad Dermatol. 2004;51(3):391-398. doi:10.1016/j.jaad.2003.12.017

12. Plewig G, ed. Braun-Falco´s Dermatology. 4th ed. Springer-Verlag GmbH; 2022.

13. Noguera-Morel L, et al. Net-like superficial vascular malformation: clinical description and evidence for lymphatic origin. Br J Dermatol. 2016;175(1):191-193. doi:10.1111/bjd.14404

14. Vide J, et al. Net-like superficial lymphatic malformation: a new entity? Clin Exp Dermatol. 2018;43(6):732-734. doi:10.1111/ced.13538

15. Iznardo H, et al. Net-like superficial lymphatic malformation. Pediatr Dermatol. 2021;38(2):516-517. doi:10.1111/pde.14526

16. Yun SJ, et al. Clinicopathological correlation of cutaneous metastatic breast carcinoma using lymphatic and vascular markers: lymphatics are mainly involved in cutaneous

metastasis. Clin Exp Dermatol. 2012;37(7):744-748. doi:10.1111/j.1365-2230.2011.04306.x

17. Bianchi R, et al. Postnatal Deletion of Podoplanin in Lymphatic Endothelium Results in Blood Filling of the Lymphatic System and Impairs Dendritic Cell Migration to Lymph Nodes. Arterioscler Thromb Vasc Biol. 2017;37(1):108-117. doi:10.1161/ATVBAHA.116.308020

18. Haining EJ, et al. Lymphatic blood filling in CLEC-2-deficient mouse models. Platelets. 2021;32(3):352-367. doi:10.1080/09537104.2020.1734784

19. Böhmer R, et al. Regulation of developmental lymphangiogenesis by Syk(+) leukocytes. Dev Cell. 2010;18(3):437-449. doi:10.1016/j.devcel.2010.01.009

20. Venot Q, et al. Targeted therapy in patients with PIK3CA-related overgrowth syndrome. Nature. 2018 Jun;558(7711):540-546. doi: 10.1038/s41586-018-0217-9.

21. Foster JB, et al. Kaposiform lymphangiomatosis effectively treated with MEK inhibition. EMBO Mol Med. 2020 Oct 7;12(10):e12324. doi: 10.15252/emmm.202012324.

22. Anderson KR, et al. Skin-Related complications of Klippel-Trenaunay Syndrome: a retrospective review of 410 patients. J Eur Acad Dermatol Venereol. 2021;35(2):517-522. doi:10.1111/jdv.16999

## FIGURES AND LEGENDS

Fig. 1

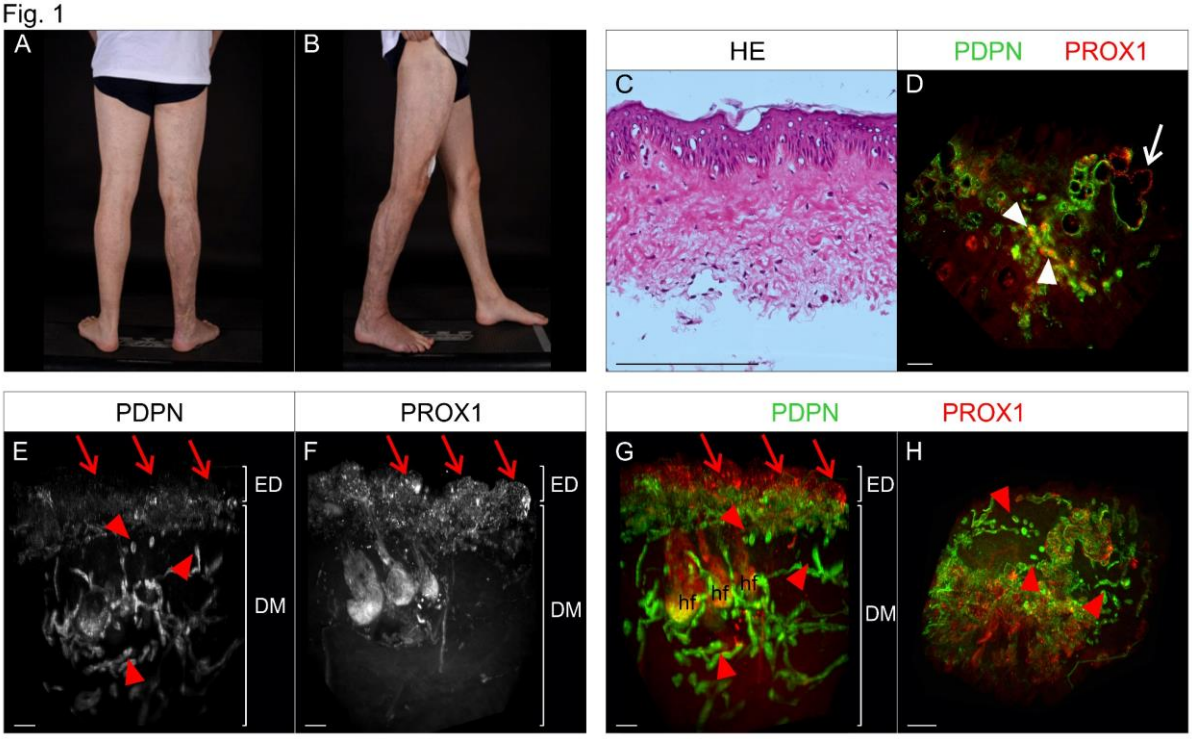


Figure 1: Macroscopic as well as 2D and 3D microscopic manifestations of a patient (Case 1) with Klippel Trenaunay Syndrome. (A, B) Patient presenting with Klippel Trenaunay syndrome with extensive venous abnormalities, dusky red port-wine birthmark, slight lymphoedema in the right leg and foot but no overgrowth. (C) Standard histological analysis of a skin biopsy from the area of the port-wine birthmark using hematoxylin & eosin stain of microtome sections. (D-H) Two-dimensional (2D) optical section (D) as well as three-dimensional (3D) reconstruction (E-H) of lymphatic vessels of wholemount immunostained affected patient tissue (port-wine birthmark) imaged using light sheet microscopy. Podoplanin (PDPN) served as a lymphatic endothelial cell-surface marker, the transcription factor PROX1 as lymphatic endothelial nuclei marker. Detected antigens and respective colours are indicated. (D) Representative 2D optical sections of wholemount immunostained affected patient tissue. Blood filled lymphatic vessels are marked by white arrow heads. PDPN negative, PROX1 positive vessels are marked by white arrow. (E-G) Maximum intensity projections of 3D reconstructed lymphatic vasculature. Visualisation of the tissue volume with the epidermis

(ED) apically, and the papillary dermis located at top and cutaneous plexus at bottom of the dermis (DM). PDPN negative, Prox1 positive cystic vascular lesions located underneath the epidermis are highlighted using red arrows. Red arrow heads: Fragmented vessels. (H) Digitally rotated view of the same specimen, showing the vessels of the papillary plexus viewed en face through the epidermis. Red arrow heads: Fragmented vessels. Hf: hair follicle. Scale bars: 200 µm.

Fig. 2

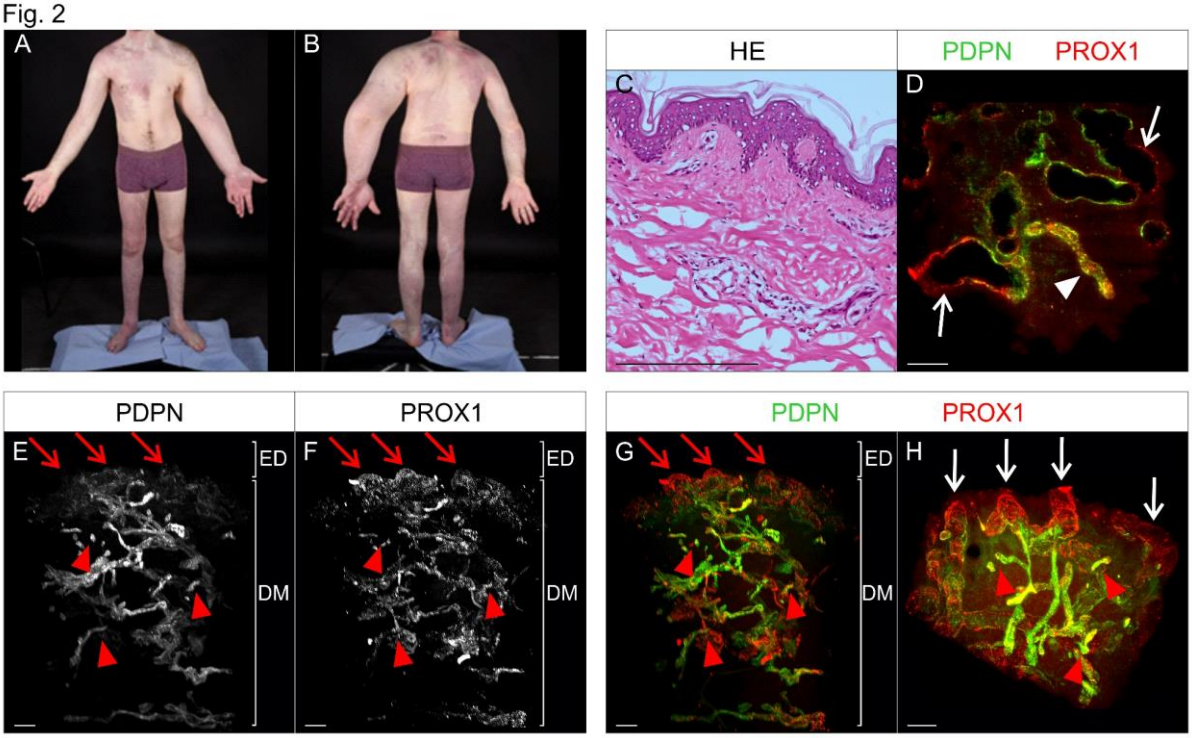


Figure 2: Macroscopic as well as 2D and 3D microscopic manifestations of a patient (Case 2) with Klippel Trenaunay Syndrome and port-wine birthmark. (A, B) Clinical manifestations of patient with Klippel Trenaunay Syndrome presenting with extensive port-wine birthmarks associated with segmental overgrowth, scoliosis, venous disease, and foot swelling. (C) Standard histological analysis of a skin biopsy with port-wine birthmark using hematoxylin & eosin stain of microtome sections. (D-H) Two-dimensional (2D) optical section (D) as well as three-dimensional (3D) reconstruction (E-H) of lymphatic vessels of wholemount immunostained affected patient tissue (port-wine birthmark) imaged using light sheet microscopy. Podoplanin (PDPN) served as a lymphatic endothelial cell-membrane marker, the transcription factor PROX1 as lymphatic endothelial nuclei marker. Detected antigens and respective colours are indicated. (D) Representative 2D optical sections of wholemount immunostained affected patient tissue. Blood filled lymphatic vessel is marked by white arrowhead. Dilated PDPN negative, PROX1 positive vessels are marked by white arrows. (E-G) Maximum intensity projections of 3D reconstructed lymphatic vasculature. Visualisation of the tissue volume with the papillary dermis located at top and cutaneous plexus at bottom of

dermis (DM). PDPN negative, Prox1 positive cystic vascular lesions located underneath the epidermis (ED) are highlighted using red arrows. Red arrowheads: Fragmented vessels. H) Digitally rotated view of the same specimen, showing the vessels of the papillary plexus viewed en face through the epidermis. White arrows: Prox1 positive, PDPN negative cystic vascular lesions. Red arrow heads: Fragmented vessels. Scale bars: 200 µm.

Fig. 3

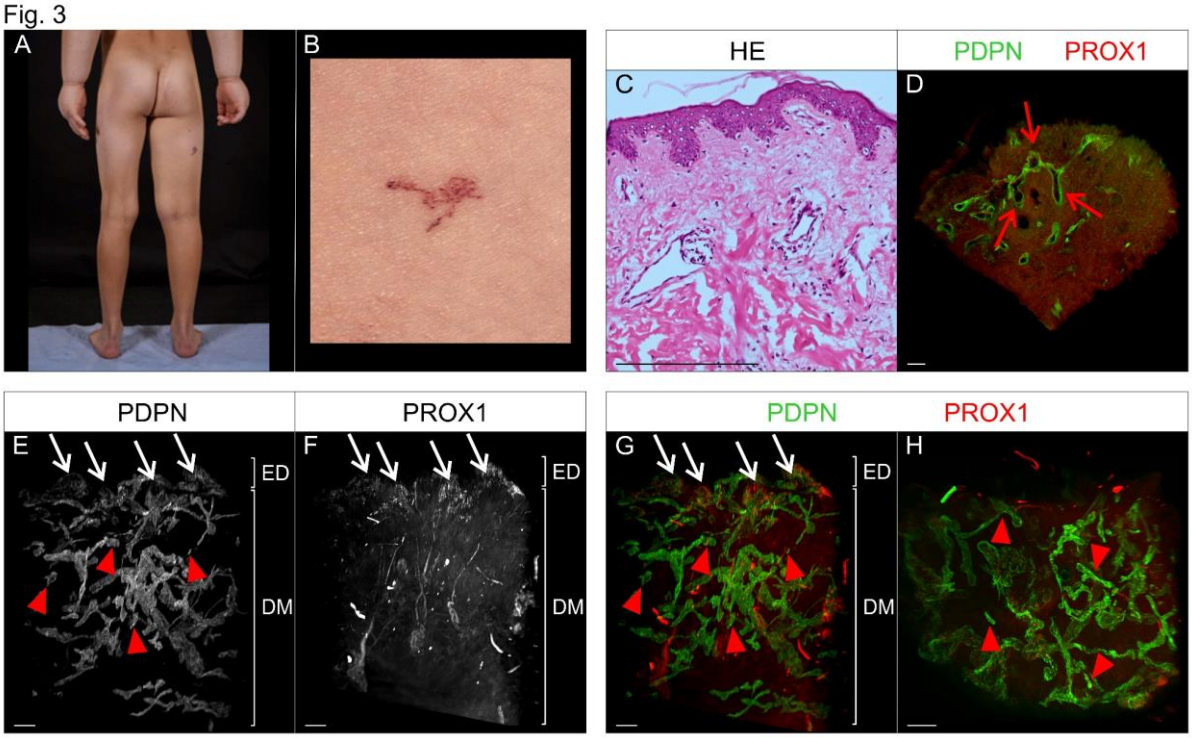


Figure 3: Macroscopic as well as 2D and 3D microscopic manifestations of a patient (Case 3) with WILD syndrome, a widespread congenital lymphedema. (A, B) Clinical manifestations of patient presenting with swollen 'boxing glove' hands, right thigh lymphoedema, and dark erythematous telangiectasia on back and side of thigh. (C) Standard histological analysis of a skin biopsy with telangiectasia using hematoxylin & eosin stain of microtome sections. (D-H) Two-dimensional (2D) optical section (D) as well as three-dimensional (3D) reconstruction (E-H) of lymphatic vessels of wholemount immunostained affected patient tissue (telangiectasia) imaged using light sheet microscopy. Podoplanin (PDPN) served as a lymphatic endothelial cell-membrane marker, the transcription factor PROX1 as lymphatic endothelial nuclei marker. Detected antigens and respective colours are indicated. (D) Representative 2D optical sections of wholemount immunostained affected patient tissue. Dilated lymphatic vessels are marked by red arrows. (E-G) Maximum intensity projections of 3D reconstructed lymphatic vasculature. Visualization of the tissue volume with the papillary dermis located at top and cutaneous plexus at bottom of dermis (DM). PDPN negative, Prox1 positive dilated vessels are highlighted using white arrows. Red arrow heads: Fragmented

vessels. H) Digitally rotated view of the same specimen, showing the vessels of the papillary plexus viewed en face through the epidermis. Red arrow heads: Fragmented vessels. Scale bars: 200 µm.

Fig. 4

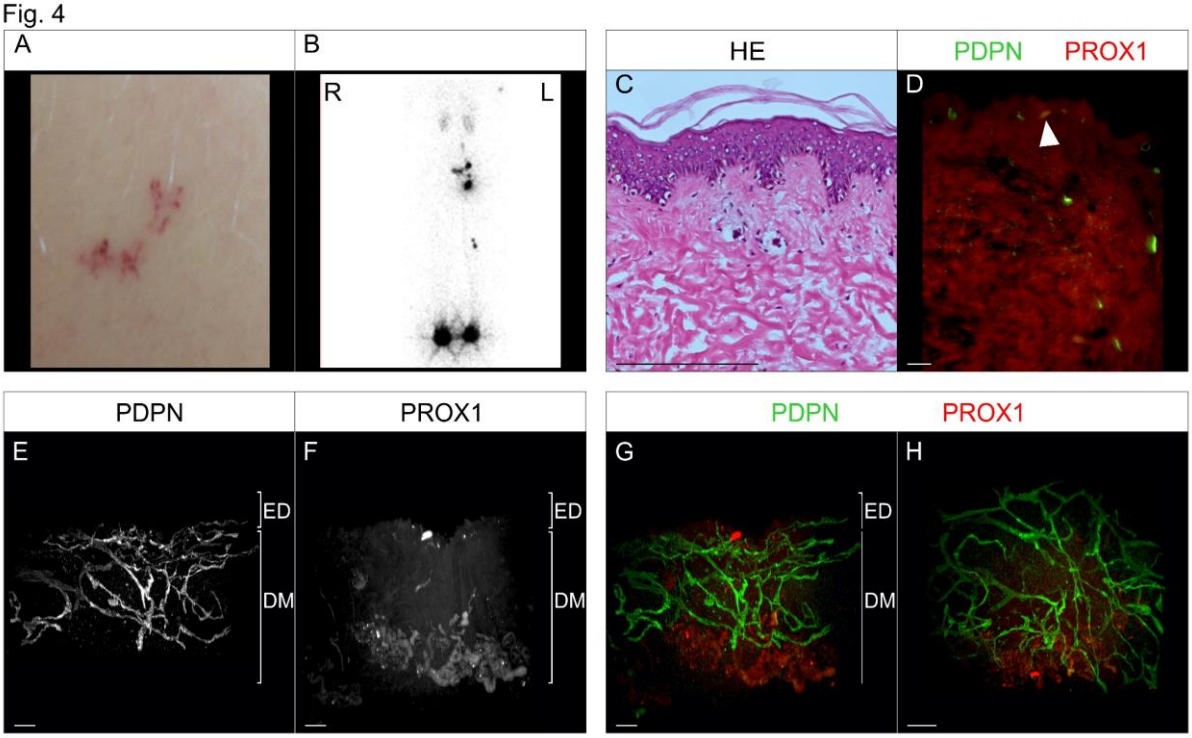


Figure 4: Macroscopic as well as 2D and 3D microscopic manifestations of a patient (case 4) with WILD syndrome and erythematous telangiectasia. (A) Telangiectasia in the skin of swollen left thigh. (B) Lymphoscintigraphy showing a posterior-anterior image with no visible tracer drainage in the left leg, but uptake in the right popliteal nodes indicating deep lymph drainage, which is an abnormal finding despite a normal leg clinically. (C) Standard histological analysis of a skin biopsy with telangiectasia using hematoxylin & eosin stain of microtome sections. (D-H) Two-dimensional (2D) optical section (D) as well as three-dimensional (3D) reconstruction (E-H) of lymphatic vessels of wholemount immunostained affected patient tissue (telangiectasia) imaged using light sheet microscopy. Podoplanin (PDPN) served as a lymphatic endothelial cell-membrane marker, the transcription factor PROX1 as lymphatic endothelial nuclei marker. Detected antigens and respective colours are indicated. (D) Representative 2D optical sections of wholemount immunostained affected patient tissue. Blood-filled lymphatic vessels are marked by white arrowhead. (E-G) Maximum intensity projections of 3D reconstructed lymphatic vasculature. Visualization of the tissue volume with the papillary dermis located at top and cutaneous plexus at bottom of

the dermis (DM). H) Digitally rotated view of the same specimen, showing the vessels of the papillary plexus viewed en face through the epidermis. Scale bars: 200 µm.

Fig. 5

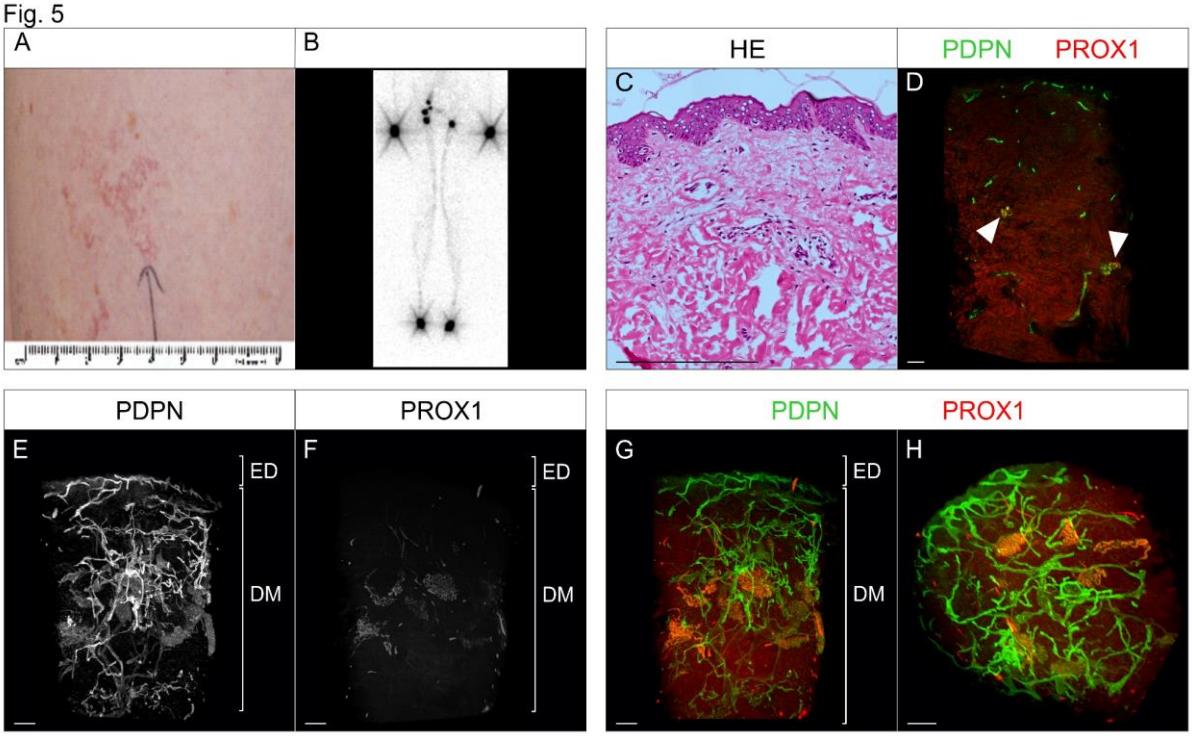


Figure 5: Macroscopic as well as 2D and 3D microscopic manifestations of a patient (case 5) with WILD syndrome and erythematous telangiectasia. (A) Clinical manifestations of patient presenting with telangiectasia in skin of left thigh from swollen limb. (B) Lymphoscintigraphy showing a posterior-anterior image showing reduced lymph node uptake of tracer in the left groin but otherwise normal looking lymph drainage pathways in both legs. (C) Standard histological analysis of a skin biopsy with telangiectasia using hematoxylin & eosin stain of microtome sections. (D-H) Two-dimensional (2D) optical section (D) as well as three-dimensional (3D) reconstruction (E-H) of lymphatic vessels of wholemount immunostained affected patient tissue (telangiectasia) imaged using light sheet microscopy. Podoplanin (PDPN) served as a lymphatic endothelial cell-membrane marker, the transcription factor PROX1 as lymphatic endothelial nuclei marker. Detected antigens and respective colours are indicated. (D) Representative 2D optical sections of wholemount immunostained affected patient tissue. Blood-filled lymphatic vessels are marked by white arrowheads. (E-G) Maximum intensity projections of 3D reconstructed lymphatic vasculature. Visualization of the tissue volume with the papillary dermis located at top and cutaneous plexus at bottom of

the dermis (DM). H) Digitally rotated view of the same specimen, showing the vessels of the papillary plexus viewed en face through the epidermis. Scale bars: 200 µm.

Fig. 6

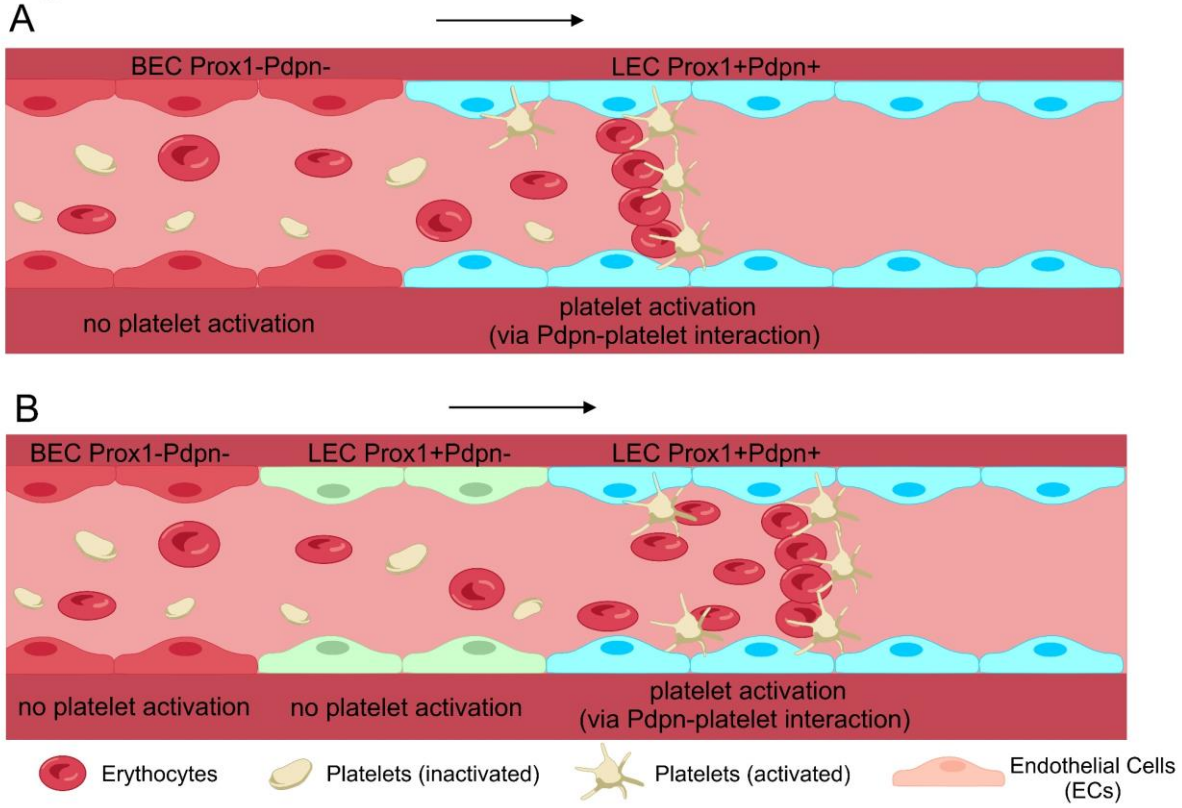


Figure 6: Schematic representation of hypothesized mechanism leading to blood filled lymphatic vessels. (A) In contrast to blood endothelial cells (BECs), lymphatic endothelial cells (LECs) lining lymphatic vessels express the lymphatic markers PROX1 and PDPN (blue LECs, right). PDPN, a surface protein, binds platelets resulting in their activation, which enables them to bind any red blood cells entering the lymphatic vessel. It is assumed that under normal physiological conditions if a shunt appear between a blood vessel and a lymphatic vessel in the skin, blood with all its components (including red blood cells and platelets) can escape into the lymphatic vessels. However, due to the immediate Podoplanin activation of the platelets, red blood cells will be bound and filling of the lymphatic vessels with red blood cells is prevented. (B) In the hypothesized model, if a shunt appears between a blood vessel and a lymphatic vessel which do not express PDPN (green LECs, middle), the platelets entering the lymphatics are not activated and therefore will not bind the entering red blood cells. This way blood filling of the lymphatic capillaries can happen, which make them appear as a

erythematous cutaneous capillary malformation (naevus). Arrow, direction of flow of red blood cells/blood.

**Table 1: Summary of phenotype and histological findings.** Overview of the phenotype of the five cases included in this study. The findings summarised for 2D optical sections and 3D reconstructions relate to the lymphatic vessel network.

| Case | Phenotype | Naevus flammeus | Telangiectasia | Persistent lymphoedema | Overgrowth | Varicose veins | Cutaneous lymphangiectasia | Cutaneous vascular lesion | Lymphoscintigraphy | 2D optical sections | 3D histological reconstruction |
|---|---|---|---|---|---|---|---|---|---|---|---|
| **1** | KTS | Right leg from ankle to groin | No | Right leg | Yes | Yes | No | No | Mild abnormalities of lymphatic function | Blood filled, dilated vessels | Dilated, fragmented vessels and cystic lesions |
| **2** | KTS | Both legs, upper torso, right upper arm and neck | No | Slightly swollen foot | Yes | Yes | No | No | | Blood filled, dilated vessels | Dilated, fragmented vessels and cystic lesions |
| **3** | WILD | No | Right thigh | Bilateral upper limbs, right thigh, genital | No | No | Yes | No | | Dilated vascular lumens | Hyperplastic, dilated vessels, no valves detected |
| **4** | WILD | No | Left thigh | Left leg extending into the left flank and buttock | No | No | No | Both sides of the neck | Functional aplasia in the affected leg | Blood filled vessels | Normal network, low number of valves |
| **5** | WILD | No | Left thigh | Left lower limb, left upper limb, left side of face | No | No | No | Left side of the chest | Reduced uptake in affected leg | Blood filled vessels | Normal network, low number of valves |

KTS, Klippel-Trenauny syndrome; WILD, Warts-Immunodeficiency-Lymphoedema-and-anogenital-Dysplasia syndrome